Langmuir

Article

pubs.acs.org/Langmuir

Adsorption and Solution Properties of Bottle-Brush Polyelectrolyte Complexes: Effect of Molecular Weight and Stoichiometry

Alexander Shovsky,[†] Imre Varga,[†,∥] Ričardas Makuška,[‡] and Per M. Claesson*[,†,§]

[†]School of Chemical Science and Engineering, Department of Chemistry, Surface and Corrosion Science, KTH Royal Institute of Technology, Drottning Kristinas väg 51, SE-100 44 Stockholm, Sweden

[‡]Department of Polymer Chemistry, Vilnius University, Naugarduko 24, LT-03225 Vilnius, Lithuania

[§]YKI, Institute for Surface Chemistry, P.O. Box 5607, SE-114 86 Stockholm, Sweden

[∥]Institute of Chemistry, Eötvös University, P.O. Box 32, 1518 Budapest 112, Hungary

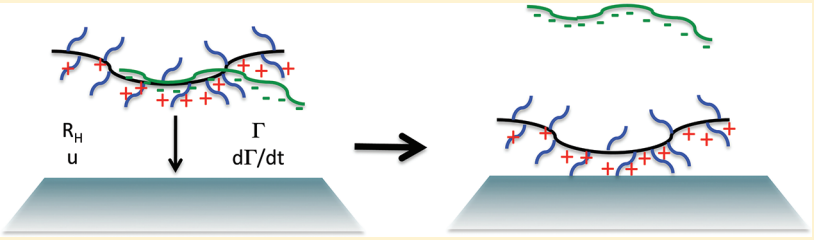

ABSTRACT: Polyelectrolyte complexes (PECs) self-assembled from bottle-brush polyelectrolytes, having a cationic main chain and uncharged side chains, and linear anionic sodium polystyrenesulfonate (NaPSS) have been investigated with emphasis on (i) the charge density and side chain density of the bottle-brush polyelectrolyte, (ii) the molecular weight of NaPSS, and (iii) the charge stoichiometry of the mixture. Light scattering and electrophoretic mobility data demonstrate that small molecular complexes are formed when the PEO_{45} side chain density is sufficiently high to provide steric stabilization and prevent PEC aggregation. The adsorption of PECs on negatively charged silicon oxynitride was investigated using dual polarization interferometry, and the time evolution of the adsorbed amount and thickness was determined. Cationic, uncharged, and negatively charged complexes all adsorb to negatively charged silicon oxynitride, and maximum adsorption is achieved for positively charged complexes containing small amounts of PSS. The adsorbed amount and the kinetics of adsorption are reduced with increasing PSS content, and for any given stoichiometry with increasing PSS molecular weight. These findings are discussed in terms of the PEC structure and the ability of anionic polyelectrolytes to leave the PECs during adsorption.

INTRODUCTION

Polyelectrolyte complexes (PECs) are spontaneously formed when polyanions and polycations are mixed in aqueous solution.[1,2] The self-assembly process is driven by the entropy gain due to counterion release,[3] and can occur in less that 5 ms as shown by stopped-flow measurements.[4] The structure and physicochemical properties of the PECs can be remarkably different from those of conventional polyelectrolytes.[5−7] Due to the predominance of strong electrostatic interactions, PECs are prone to be trapped in nonequilibrium states; that is, the experimental protocol (polyelectrolyte concentration, rate of addition and mixing order) can affect PEC properties.[8,9]

Complex formation between oppositely charged polyelectrolytes has attracted considerable interest, partly due to the use of PECs in a wide range of applications. PECs have found use as flocculants,[10] binders,[11] and coatings,[12] as well as in water purification, wastewater treatment,[13,14] and papermaking.[15,16] More recently, PECs have also been successfully employed in biomedical applications,[17] such as gene therapy and drug delivery,[18] protein separation,[19] and microencapsulation.[20] In most applications, PECs are used in the form of aqueous dispersions that experience contact with a (charged) surface. Hence, it is crucial to understand and control both PEC dispersions and adsorption of PECs at solid−liquid interfaces.

Depending on the charge ratio between the two polyelectrolytes in solution, insoluble stoichiometric complexes or soluble nonstoichiometric complexes can be prepared. Systematic studies of the formation and structure of nonstoichiometric PECs have been reported by the groups of Tsuchida,[21] Lunkwitz,[22] Dautzenberg,[23,24] and Kabanov,[9,25] and computer simulations performed by Linse[26−28] and Khokhlov[29,30] have increased our fundamental understanding significantly. The nonstoichiometric PECs fall into two categories: (i) highly aggregated complexes consisting of several polyelectrolyte chains that are stabilized by the polyion in excess. These particles consist of a neutralized, relatively compact core and a surrounding shell of the excess component that stabilizes the PEC particles by electrostatic repulsion. (ii) Water-soluble molecular complexes that form when special conditions are met.[27]

Received: January 27, 2012
Revised: April 2, 2012
Published: April 3, 2012

   dx.doi.org/10.1021/la300365q | *Langmuir* 2012, 28, 6618−6631

Stoichiometric complexes contain equivalent amounts of the oppositely charged units, and they are therefore electroneutral. They are usually insoluble and precipitate out of solution.[1] However, the precipitation of stoichiometric PECs can be prevented if a hydrophilic nonionic block (e.g., poly(ethylene oxide), PEO) is attached to at least one of the polyelectrolytes.[31−33] In such a case, uncharged water-soluble PECs are formed, composed of a water insoluble core (the insoluble PEC) surrounded and stabilized by a hydrophilic PEO corona. Bottle-brush polyelectrolytes,[34] with a charged backbone and hydrophilic PEO side chains, provide an alternative route to prepare water-soluble stoichiometric PECs with oppositely charged linear polyelectrolytes.[35−38]

The above-mentioned bottle-brush structure, with a charged backbone and uncharged side chains, is reversed to what is found in nature where charged side chains are attached to a main chain in molecules such as mucin, aggrecan, and lubricin that alone and in complexes with, for example, phospholipids fulfill important biological functions of protection and lubrication.[39,40] Molecular bottle-brush polymers have interesting properties, particularly when the side chains are stimuli-responsive,[41] and the self-assembly between bottle brushes with ionic side chains and other compounds have been investigated. For instance, association with oppositely charged organic multivalent ions,[42] surfactants,[43] latex particles,[44] and polyelectrolytes[45,46] have been reported.

The adsorption of polyelectrolytes as a function of polyelectrolyte molecular weight has been considered in several studies.[47,48] Likewise, several studies on solution properties of PECs can be found. However, their adsorption properties have received much less attention,[49] and only a few recent reports are concerned with molecular weight effects.[50] In this Article, we consider the formation of colloidally stable stoichiometric and nonstoichiometric PEC particles formed by cationic bottle-brush polyelectrolytes, having a charged main chain and uncharged side chains, and linear anionic polyelectrolytes with different molecular weight. We report how the charge density of the bottle-brush polyelectrolyte and the polyanion molecular weight, the polyelectrolyte concentration, and the complex stoichiometry affect the PEC particles formed in solution and their adsorption properties. The properties of dispersed stoichiometric and nonstoichiometric PECs were determined by dynamic light scattering and by electrophoretic mobility measurements. The adsorption of PECs on silicon oxynitride was investigated using dual polarization interferometry, DPI. The adsorption kinetics and the physical characteristics of the adsorbed layers were determined from the DPI measurements. The results provide insights into the mechanism of PEC adsorption and the structure of the adsorbed layer.

MATERIALS AND METHODS

Materials. Sodium poly(styrenesulfonate), NaPSS, standards (M_w = 4.3, 17, 70, 150 kDa, M_w/M_n = 1.1) were purchased from Fluka and used as received. Copolymers of methacryloxyethyl trimethyl ammonium chloride, METAC, and poly(ethylene oxide) methyl ether methacrylate, PEO_{45}MEMA, with three distinct molar ratios were synthesized by free-radical copolymerization as reported previously.[51] This results in close to random copolymers, having a M_w/M_n ratio of around 2−3, typical for polymers prepared by this method. Henceforth, PEO_{45}MEMA:METAC-X represents the general abbreviation of these bottle-brush copolymers. The subscript 45 refers to the number of ethylene oxide units in the side chains, and X denotes the molar percentage of charged units in the main chain (X = 75, 50, 25 in this study). The molecular weights, M_w, for the cationic bottle-brush polymers with X = 75, 50, and 25 are 520, 680, and 660 kDa, respectively. The molecular structures of the segments are schematically depicted in Figure 1. The short and linear polyanion, NaPSS, is composed of only one type of segment as illustrated in Figure 1a. The two types of segments in the bottle-brush copolymers are shown in Figure 1b and c.

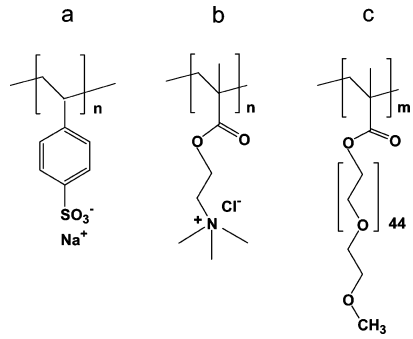

Figure 1. Schematic representation of the molecular structure of the segments in the polyelectrolytes used: (a) NaPSS, (b) METAC, and (c) PEO_{45}MEMA.

The water used in all experiments was first pretreated with a Milli-RO 10 Plus unit and then further purified with a Milli-Q PLUS 185 system. The resistivity after the treatment was 18.2 MΩ cm, and the total organic carbon content of the water did not exceed 2 ppb. Sodium chloride (analytical grade) was purchased from Fluka.

Dynamic Light Scattering. Dynamic light scattering, DLS, measurements were conducted with a Brookhaven Instruments device, which consists of a BI-200SM goniometer and a BI-9000AT digital autocorrelator. A water-cooled argon-ion laser, Lexel 95 model 2, was used as light source. The laser was used at a wavelength of 514.5 nm and emitted vertically polarized light at a maximum power of 840 mW. In DLS mode, the signal analyzer was used in a "multi tau" mode, that is, the time axis was logarithmically spaced to span the required correlation time range. The autocorrelation functions were measured at an angle of 90° in 218 channels using a 100 μm pinhole size.

The measured autocorrelation functions were analyzed by the CONTIN and the second-order cumulant methods. The samples were found to be polydisperse, having a wide monomodal size distribution. The autocorrelation function $g^1(q,\tau)$ is in the cumulant expansion given by

$$g^1(q,\tau) = \exp(-\Gamma\tau)\left(1 + \frac{\mu_2}{2}\tau^2 - \ldots\right) \quad (1)$$

where q is the scattering vector, τ the correlation time, Γ the first cumulant, and μ_2 the second cumulant. Despite the polydispersity of the samples, the mean hydrodynamic diameter (the first cumulant of the second order cumulant expansion) is used for the presentation of the changes in the hydrodynamic size distribution. For polydisperse systems, the first cumulant represents the z-average of the diffusion coefficient,[52] and a polydispersity index, PDI, is defined by the relation:[53]

$$\mathrm{PDI} = \frac{\mu_2}{\Gamma^2} \quad (2)$$

At finite concentrations and q-values, an apparent diffusion coefficient, $D_{app} = \Gamma/q^2$, is obtained, and by using the Einstein−Stokes equation the apparent hydrodynamic radius of the PEC particles can be determined.

$$D_{app} = \frac{k_B T}{f} = \frac{k_B T}{6\pi\eta R_H} \quad (3)$$

Here, k_B is the Boltzmann constant, T the absolute temperature, f the drag coefficient, η the viscosity of the medium, and R_H the hydrodynamic radius. The autocorrelation functions were analyzed

dx.doi.org/10.1021/la300365q | Langmuir 2012, 28, 6618−6631

with the software supplied by Brookhaven Instruments. The results of 30 consecutive measurements were averaged for each PEC sample.

Electrophoretic Mobility Measurements. The electrophoretic mobility of the aggregates was determined using a Zetasizer 2000 device (Malvern Instruments, U.K.) in 5 mM NaCl solution at 25 °C. The instrument was calibrated prior to measurements using Malvern zeta potential transfer standard (code DTS-1050).

Dual Polarization Interferometry. DPI allows measurements of thickness and refractive index of adsorbed layers in situ and in real time. The instrument used was an AnaLight Bio200 from Farfield Sensors Ltd. (Manchester, U.K.). The instrument consists of a helium−neon laser (emitting light at 632.8 nm), a means to select plane-polarized light, a sensor constructed using two optical waveguides stacked one on the top of each other, and a camera. A detailed description of the instrument is provided by Swann et al.[54] The substrate surface is a sandwich-like chip structure of two horizontally stacked waveguides made of silicon oxynitride, that is, nitrogen-doped silica. This substrate is preferred due to its excellent optical properties with low absorption losses in the visible and near IR region combined with a high refractive index (about 1.5). Silicon oxynitride has an isoelectric point at pH 3, and we have determined the zeta potential in 1 mM KCl solutions at pH 6 to about −50 mV using streaming potential measurements. When plane-polarized laser light is shone on the short end of the surface, it splits and travels separately through the two waveguides (sensing and reference). As the light emerges on the other side of the chip, a camera in the far field detects the resulting interference pattern. The evanescent field emitted from the sensing waveguide into the solution is affected by changes in the refractive index profile above the sensing waveguide, thus both changes in bulk solution and adsorption affects the response. Hence, the light propagating through the sensing waveguide is somewhat changed relative to the light traveling through the reference waveguide. This difference is detected as a shift in the fringe pattern in the far field, and these shifts are alternately and continuously recorded for both horizontally and vertically polarized light. By assuming formation of a homogeneous and isotropic adsorption layer, a unique solution for the thickness and refractive index of the layer can be calculated from the measured DPI signals.[55] The adsorbed mass was calculated using eq 4 and the refractive index increments, dn/dc, previously reported:[56]

$$\Gamma = \frac{d_f(n_f - n_{buffer})}{\frac{dn}{dc}} \tag{4}$$

A 100 μm thick silicon mask with two slits is placed on top of the waveguide chip. As the chip is mounted in the instrument, these two slits create two separate flow channels, which constitute the measurement chambers. Solution is continuously flowed through the channels by use of a syringe pump (model PHD200, Harvard Apparatus). The samples are injected through an HPLC valve and can be directed to flow through both or just one of the two channels. Before the adsorption is started, the instrument and the waveguide are calibrated by injecting two solutions of known index of refraction, in this case aqueous 5 mM NaCl and ethanol (80%).

The DPI chip surface was cleaned by using the following steps: (i) dipping in a (1:1) mixture of HCl (37%) and CH_3OH (abs) for 15 min, (ii) rinsing with water, (iii) dipping in a 2 wt % surfactant-free Deconex 20 NS (Fisher Scientific) for 15 min, (iv) rinsing with water, and (iv) finally it was kept in water for 12 h. The chip surface was prior to measurements additionally cleaned by injection of Deconex 20 NS (2%) for 20 min followed by rinsing with water until stable DPI signals were achieved (30 min). We found that this cleaning procedure provided hydrophilic surfaces and results with good reproducibility.

Experimental Procedures. Stock solutions of the polycations with a concentration of 5000 ppm were prepared in 5 mM NaCl. NaPSS stock solutions were prepared in 5 mM NaCl in such a manner that the concentrations of the anionic charges from PSS were equal to the concentrations of cationic charges from the bottle-brush polyelectrolytes in their stock solutions. The polyelectrolyte stock solutions were vigorously stirred for ∼24 h, and thereafter filtered employing a 0.1 μm inorganic membrane filters (Whatman, Anotop 25). All dilutions were made using 5 mM NaCl, and all samples were prepared at room temperature (∼25 °C).

The PECs were formed by means of an automatic mixing process, using a programmable infusion pump (model PHD200, Harvard Apparatus). Mixing was achieved by simultaneous injection of the two polyelectrolyte solutions (2.5 cm^3 of each) via small diameter tubes (d = 1 mm) into 5 cm^3 of continuously stirred 5 mM NaCl solution. The applied infusion rate was 1 cm^3/min. The final volume of the PEC containing solution was 10 cm^3. Solutions with stoichiometric ratios (5:1), (2:1), (1:1), (1:2), and (1:5) between cationic groups from PEO_{45}MEMA:METAC-X and anionic groups from NaPSS were investigated.

For DPI measurements, solutions of PECs were freshly prepared to contain a concentration of cationic bottle-brush polymer of 100 ppm. The concentrations were then adjusted to 10, 20, and 50 ppm by using aqueous 5 mM NaCl solution. The PEC solutions were injected into the measurement cell, and the adsorption process was followed in real time. The rinsing buffer was aqueous 5 mM NaCl solution. The flow rate used in our experiments was 50 μL/min, and all measurements were carried out at 20 °C.

RESULTS

Mixing low concentrations (50−200 ppm) of PEO_{45}MEMA:METAC-75 with $NaPSS_x$, where the subscript "x" represents different molecular weights of PSS, results in formation of solutions with low turbidity. The turbidity increases progressively as the polyelectrolyte concentration increases, indicating formation of large aggregates due to increased polyelectrolyte collision frequency. In contrast, the stoichiometric and non-stoichiometric mixing of PEO_{45}MEMA:METAC-50 or PEO_{45}MEMA:METAC-25 with $NaPSS_x$ leads to formation of optically transparent solutions, regardless of the PSS molecular weight. In these cases, increase in polyelectrolyte concentration causes no visible effect on the optical properties of the mixtures, indicating formation of small PECs.

Charge Characteristics of Polyelectrolyte Complexes. The electrophoretic mobility, mean values, and standard deviation of these values from 15 experiments for PEO_{45}MEMA:METAC-25/PSS_x and PEO_{45}MEMA:METAC-50/PSS_x PECs are shown as a function of the ratio [PSS charges]/([METAC charges] + [PSS charges]) in Figure 2. As expected, the sign of the mobility of the PEC particles corresponds to the sign of the component in excess, and the mobility at the stoichiometric ratio (0.5) is close to zero. Regardless of the molecular weight of PSS, a further increase in PSS content results in increased negative electrophoretic mobility of the complexes.

The measured electrophoretic mobility, u, is influenced by the charge, Q, of the PEC particles and by their size. The number of elementary charges, z, contributing to the electrophoretic mobility of the complex can, without any assumption of particle size or shape, be estimated using the Einstein relation according to

$$z = \frac{uk_BT}{eD} \tag{5}$$

where e is the elementary charge and D is the diffusion coefficient. The number of charges from small ions that are hydrodynamically associated with the PECs, z_H, can be determined using the relation $z_H = (z_{tot} - z)$, where z_{tot} is the total number of charges calculated based on the molecular composition of the polyelectrolytes.

$$z_{tot} = z_B(1 - r) \tag{6}$$

dx.doi.org/10.1021/la300365q | Langmuir 2012, 28, 6618−6631

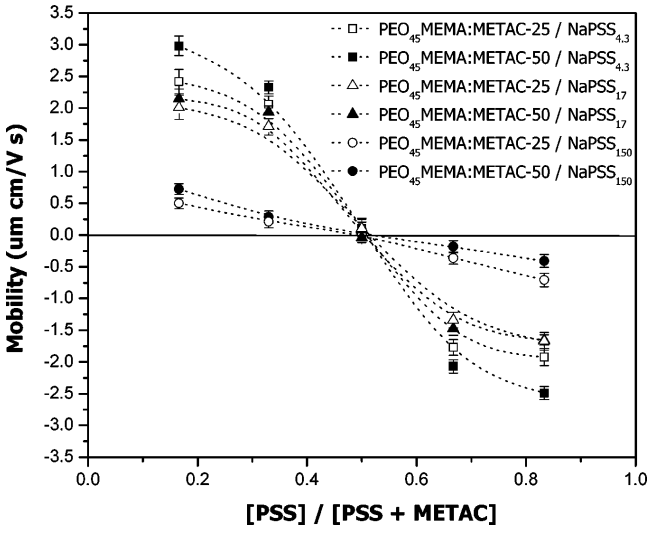

Figure 2. Electrophoretic mobility vs PSS content for $PEO_{45}MEMA$:-METAC-50/$NaPSS_x$ and $PEO_{45}MEMA$:METAC-25/$NaPSS_x$. The concentration of the cationic polymer was fixed to 50 ppm. The horizontal line represents zero mobility. Each data point represents measurements performed on separately prepared PEC samples.

where z_B is the charge of the bottle-brush polymer and r is the charge ratio [PSS charges]/[METAC charges] in the mixture. Numerical values for u, D, z, and z_H are summarized in Table 1.

For any given charge stoichiometry of the mixture, the electrophoretic mobility of the PECs decreases with the molecular weight of PSS. This is partly due to an increased size of the PEC particles, as demonstrated by dynamic light scattering measurements (see below). Further, the absolute values for the mobility of positively and negatively charged $PEO_{45}MEMA$:METAC-25/PSS_x complexes were found to be somewhat lower compared to the mobility determined for $PEO_{45}MEMA$:METAC-50/$NaPSS_x$ PECs with the same stoichiometric ratio. This is in line with the lower number of charges and higher number of PEO_{45} side chains in $PEO_{45}MEMA$:METAC-25/PSS_x complexes as compared to $PEO_{45}MEMA$:METAC-50/PSS_x.

Hydrodynamic Size of Polyelectrolytes and Polyelectrolyte Complexes. *Polyelectrolytes.* The z-average hydrodynamic radii, R_H, of the polyelectrolytes and the PECs were calculated from eq 3 using diffusion coefficients determined by DLS measurements in aqueous 5 mM NaCl solution. The R_H-values for $PEO_{45}MEMA$:METAC-25, $PEO_{45}MEMA$:-METAC-50, and $PEO_{45}MEMA$:METAC-75 were 15, 17, and 22 nm respectively, which agrees well with data previously reported.[37,38] The hydrodynamic sizes for the anionic $NaPSS_x$ polyelectrolytes (M_w = 17, 70, and 150 kDa) were found to be 3, 6, and 9 nm respectively. This data set for NaPSS is well described by the relation:

$$R_H = 0.023 M_w^{0.5} \quad (7)$$

where R_H is in nm and M_w in g/mol. In contrast, if an exponent of 0.6 is used, then the prefactor decreases with increasing molecular weight. The size of $NaPSS_{4.3}$ was too small to be determined by DLS measurements, even when a high concentration was used (2000 ppm). However, by using eq 7, it can be estimated to 1.5 nm.

Polyelectrolyte Complexes of $PEO_{45}MEMA$:METAC-75/PSS_x. The hydrodynamic radius of stoichiometric $PEO_{45}MEMA$:-METAC-75/PSS_x complexes as a function of polycation concentration recorded shortly after their formation (2 min) is shown in Figure 3a.

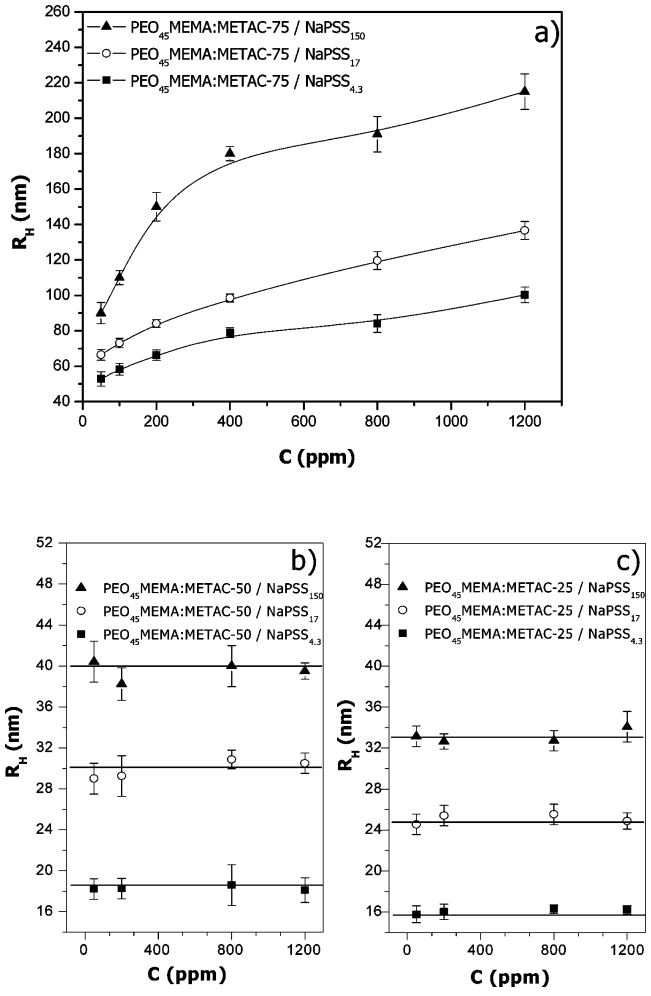

Figure 3. Hydrodynamic radius of stoichiometric (1:1) complexes containing (a) $PEO_{45}MEMA$:METAC-75, (b) $PEO_{45}MEMA$:-METAC-50, and (c) $PEO_{45}MEMA$:METAC-25 as a function of polycation concentration. The solutions contained 5 mM NaCl. The lines are plotted as guides for the eye.

Clearly, the size of the PECs increases with increasing polyelectrolyte concentration, regardless of the molecular weight of the polyanion. The effect of concentration on R_H suggests formation of PEC aggregates (assemblies of several polyanion−polycation macromolecules) rather than molecular complexes. At each concentration, R_H increases as the molecular weight of PSS is increased.

The hydrodynamic size was also determined for different nonstoichiometric $PEO_{45}MEMA$:METAC-75/PSS_x PECs. The DLS data for all nonstoichiometric compositions showed the same trend as for stoichiometric PECs, that is, R_H increases with polyelectrolyte concentration and molecular weight of the polyanion. In addition, we found that for any given concentration the hydrodynamic radius of the complexes increases with increasing PSS content, that is, in the order (1:5) ≈ (1:2) > (1:1) > (2:1) > (5:1) (data not shown).

Polyelectrolyte Complexes of $PEO_{45}MEMA$:METAC-50/PSS_x and $PEO_{45}MEMA$:METAC-25/PSS_x. The hydrodynamic size of the stoichiometric complexes formed by the lower charge

dx.doi.org/10.1021/la300365q | Langmuir 2012, 28, 6618−6631

Table 1. Solution Characteristics of Bottle-Brush Polyelectrolytes and PECs[a]

	u (10^{-8} m^2/V·s)	D_{app} (10^{-12} m^2/s)	z	$z_H = z_{tot} - z$	PDI
PEO_{45}MEMA:METAC-25	3.2	13.6	63	39	0.21
PEO_{45}MEMA:METAC-50	3.8	12.4	85	210	0.23
PEO_{45}MEMA:METAC-25/$NaPSS_{4.3}$					
0.166	2.4	12.5	50	32	0.24
0.33	2.1	13.2	40	11	0.23
0.5	0.9	12.6	2	2	0.25
0.667	−1.8	9.0	−51	−49	0.23
0.833	−1.9	8.3	−60	−350	0.22
PEO_{45}MEMA:METAC-50/$NaPSS_{4.3}$					
0.1666	2.9	11.2	66	170	0.22
0.33	2.3	12.2	51	97	0.24
0.5	0.1	11.1	5	−5	0.24
0.667	−2.1	7.9	−67	−230	0.23
0.833	−2.5	7.5	−86	−1100	0.23
PEO_{45}MEMA:METAC-25/$NaPSS_{17}$					
0.1666	2.0	10	49	32	0.25
0.33	1.7	9.9	44	7	0.24
0.5	0.1	7.9	3	−3	0.22
0.667	−1.3	5.7	−61	−140	0.24
0.833	−1.6	5.2	−80	−430	0.24
PEO_{45}MEMA:METAC-50/$NaPSS_{17}$					
0.166	2.1	7.6	72	160	0.24
0.33	1.9	7.6	66	83	0.24
0.5	0.1	6.8	2	−2	0.22
0.667	−1.5	4.8	−78	−220	0.23
0.833	−1.6	4.9	−86	−1100	0.26
PEO_{45}MEMA:METAC-25/$NaPSS_{150}$					
0.166	0.5	5.6	22	60	0.31
0.33	0.5	5.0	16	35	0.31
0.5	0.1	4.3	1	−1	0.31
0.667	−0.4	3.5	−26	−76	0.36
0.833	−0.5	3.3	−42	−370	0.37
PEO_{45}MEMA:METAC-50/$NaPSS_{150}$					
0.166	0.7	5.2	36	200	0.31
0.33	0.4	4.5	22	130	0.31
0.5	0.1	3.6	1	−1	0.33
0.667	−0.2	2.5	−19	−280	0.37
0.833	−0.4	2.2	−46	−1100	0.37

[a]The PSS content is given by the ratio of PSS charges/(METAC charges + PSS charges) in the mixture.

density bottle-brush polyelectrolytes, PEO_{45}MEMA:METAC-25 and PEO_{45}MEMA:METAC-50, with different molecular weight NaPSS at different polyelectrolyte concentrations is illustrated in Figure 3b and c, respectively. In this case, the polyelectrolyte concentration did not affect the hydrodynamic radius, indicating formation of small molecular complexes.

The hydrodynamic radius as a function of the molecular weight of NaPSS in the PECs, for different complex compositions, is reported in Figure 4a for PEO_{45}MEMA:METAC-50/PSS_x and in Figure 4b for PEO_{45}MEMA:METAC-25/PSS_x.

The data sets obtained for PECs formed with the two different bottle-brush polyelectrolytes show the same trend: increasing the molecular weight of PSS up to 70 kDa leads to pronounced increase in hydrodynamic radius of the complexes, whereas a further increase in molecular weight to 150 kDa hardly affects the hydrodynamic radius of the PECs. The size of the PEO_{45}MEMA:METAC-50 containing complexes is somewhat larger than that of the PEO_{45}MEMA:METAC-25 PECs, independent of complex stoichiometry. For both bottle-brush polyelectrolytes, at any given NaPSS molecular weight, R_H increases as the NaPSS content is increased, that is, in the order (1:5) ≈ (1:2) > (1:1) > (2:1) > (5:1). Finally, we note that the polydispersity index determined for PECs formed by small PSS anions ($M_w \leq 17$ kDa) is close to those determined for the bottle-brush polyelectrolytes, whereas larger polydispersity is determined for the PECs containing larger molecular weight PSS (Table 1).

Colloidal Stability of PECs. The colloidal stability of the stoichiometric and nonstoichiometric PECs in 5 mM NaCl was probed by repeating (daily) the light scattering measurements on stored samples under a period of 2 weeks and further at different time intervals until a total time of 3 months. The hydrodynamic size of positively charged, (5:1) (2:1), and neutral (1:1) PEO_{45}MEMA:METAC-75/PSS_x (x = 4.3, 17 kDa) complexes was found to remain constant as shown in Figure 5 for PEO_{45}MEMA:METAC-75/PSS_{17} PECs. However, the size of the negatively charged nonstoichiometric PECs increases for several days due to further aggregation until precipitation occurs and only small aggregates remain in solution (Figure 5).

dx.doi.org/10.1021/la300365q | Langmuir 2012, 28, 6618−6631

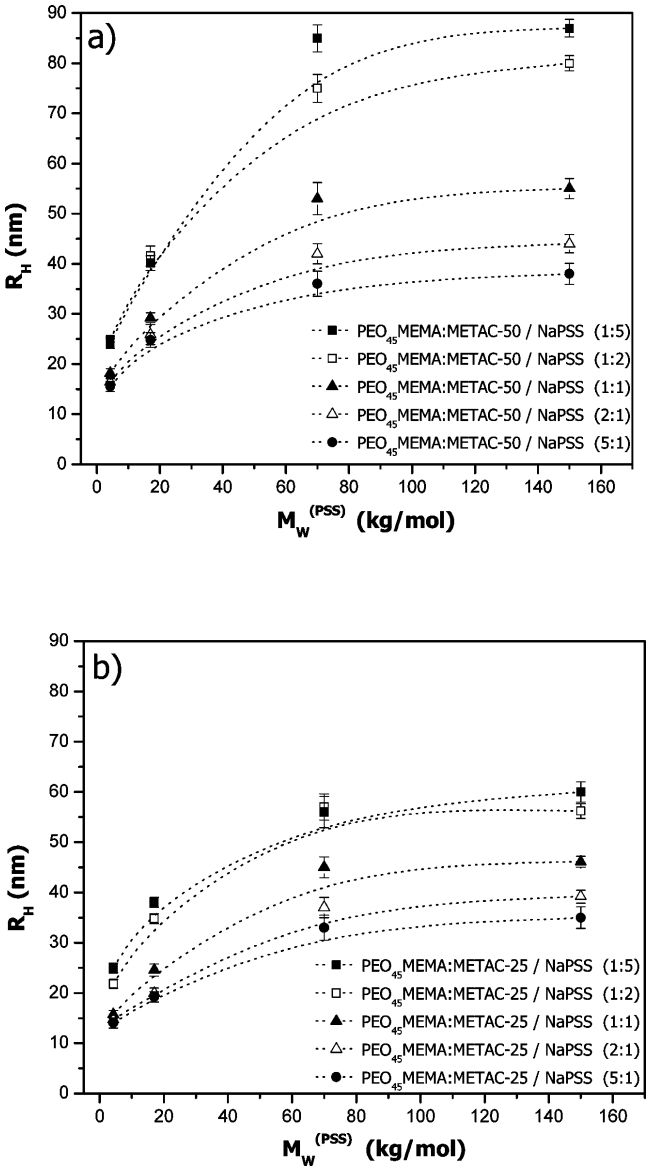

Figure 4. Hydrodynamic radius of complexes containing (a) PEO_{45}MEMA:METAC-50 and (b) PEO_{45}MEMA:METAC-25 as a function of PSS molecular mass. The solution contained 5 mM NaCl and 50 ppm of PEO_{45}MEMA:METAC-25(50). The curved lines are plotted as guides for the eye.

A similar evolution with time has been observed for mixtures of PEO_{45}MEMA:METAC-75/$PSS_{4.3}$[37] and for cationic polyelectrolytes mixed with anionic surfactants.[57,58] An increase in molecular weight of the anionic polyelectrolyte to 150 kDa promoted aggregation of the PEC particles, and in this case R_H increased during several days of storage and then decreased due to sedimentation for all stoichiometries investigated (data not shown). This demonstrates limited colloidal stability regardless of complex composition.

The hydrodynamic size of PEO_{45}MEMA:METAC-25/PSS_x and PEO_{45}MEMA:METAC- 50/PSS_x PECs, at any studied molecular weight of PSS and at any stoichiometric ratio, remained unchanged during storage for 6 months. This suggests formation of colloidally stable complexes. Addition of NaCl to these PEC solutions, up to a concentration of 0.5 M, did not cause any increase in turbidity or precipitation, which indicates that the density of uncharged PEO_{45} side chains in the bottle-brush polymer is sufficient to achieve steric stabilization of the PECs that inhibits their further aggregation to larger particles. As an illustration of this behavior, the hydrodynamic radius for PEO_{45}MEMA:METAC-25/$PSS_{4.3}$ as a function of salt concentration is illustrated in Figure 6. Clearly, the high side chain density provides an efficient steric barrier that prevents flocculation even at high ionic strength.

Adsorption of Polyelectrolytes and Polyelectrolyte Complexes. *Polyelectrolytes.* Adsorption of the different polyelectrolytes on silicon oxynitride from 5 mM NaCl was investigated with DPI. The adsorbed amounts achieved for PEO_{45}MEMA:METAC-50 and PEO_{45}MEMA:METAC-25 were 1.7 and 2.3 mg/m^2, respectively. The corresponding layer thicknesses were 5.1 nm for PEO_{45}MEMA:METAC-50 and 11.0 nm for PEO_{45}MEMA:METAC-25. No adsorption could be detected for NaPSS, independent of molecular weight.

Polyelectrolyte Complexes. Adsorption of stoichiometric and nonstoichiometric PEO_{45}MEMA:METAC-25/PSS_x and PEO_{45}MEMA:METAC-50/PSS_x complexes on silicon oxynitride surfaces was performed from aqueous 5 mM NaCl solutions. The evolution of the adsorbed mass as a function of time during the initial stage of the adsorption process for PEO_{45}MEMA:METAC-25/PSS_x and PEO_{45}MEMA:METAC-50/PSS_x (x = 17 and 150 kDa) complexes with different mixing ratios are compared in Figure 7. The adsorbed amount decreases in the order (2:1) > (1:1) > (1:2), that is, with increasing amount of anionic polyelectrolyte in the complex. We also note that the adsorbed amount obtained for positively charged complexes containing low molecular weight NaPSS (<17 kDa) is larger than that for the cationic bottle-brush polyelectrolyte alone, whereas cationic complexes containing NaPSS with M_w = 17 kDa adsorb to about the same extent as the bottle-brush polyelectrolyte. For PECs with high molecular weight NaPSS (M_w = 150 kDa), the adsorption of the cationic PECs is significantly lower than that for the bottle-brush polyelectrolyte alone. Furthermore, regardless of the PEC composition, PEO_{45}MEMA:METAC-25 containing complexes adsorbed in larger amounts on silicon oxynitride compared to complexes containing the higher charge density bottle-brush polymer PEO_{45}MEMA:METAC-50.

It is also of interest to consider the initial adsorption kinetics, as evaluated from the initial slope of the curves shown in Figure 7. The DPI microfluidic flow chamber is designed after the biosensor thin layer cell described by Glaser[59] with well-characterized mass-transfer characteristics in a parabolic laminar flow profile.[60] For this situation, the flux of polymer, j, from the bulk to the surface is described by eq 8. The concentration c_b equals the polymer concentration of the injected solution while, c_s is the concentration of nonadsorbed polymers adjacent to the surface.

$$j = k_m(c_b - c_s) \tag{8}$$

which in the initial state of adsorption simplifies to

$$j = k_m c_b \tag{9}$$

The value of k_m can, if all molecules that reach the surface adsorb, be determined from the initial slope of the adsorption curves $(d\Gamma/dt)_{t\to 0}$ illustrated in Figure 7. Theoretically, it is given by[60]

$$k_m = C\sqrt[3]{\frac{D_{app}{}^2 F}{h^2 wl}} = \left(1.26 \times 10^{-7}\right)\sqrt[3]{D_{app}{}^2} \tag{10}$$

dx.doi.org/10.1021/la300365q | Langmuir 2012, 28, 6618−6631

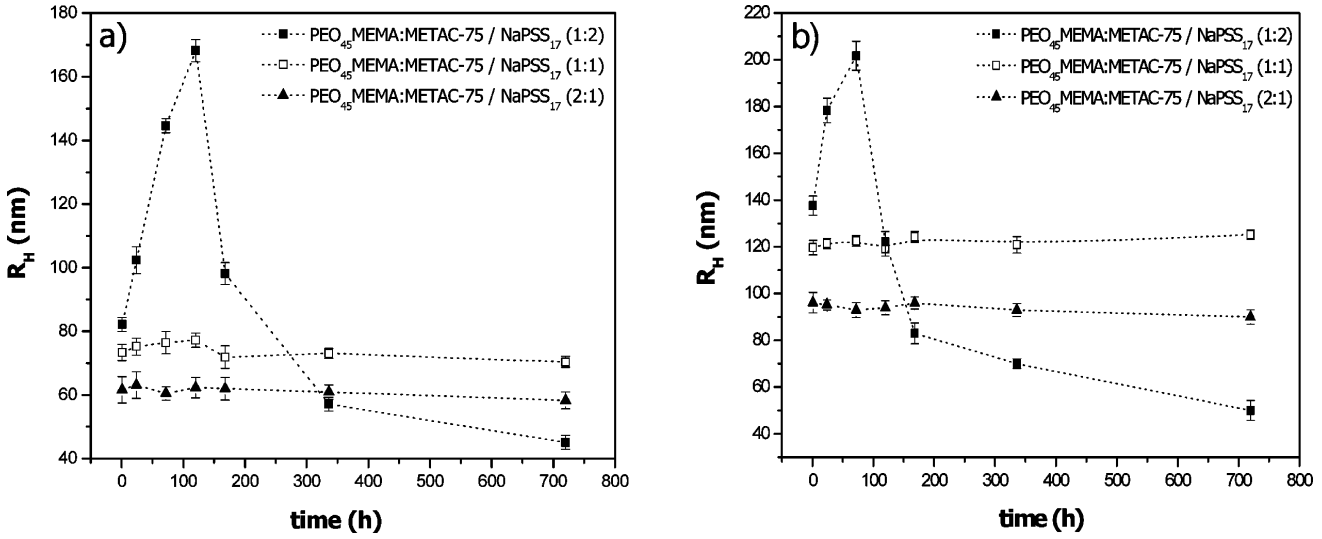

Figure 5. Hydrodynamic radius of complexes containing PEO_{45}MEMA:METAC-75 as a function of time (a) 100 ppm and (b) 1000 ppm. The solution contained 5 mM NaCl. The lines are plotted as guides for the eye.

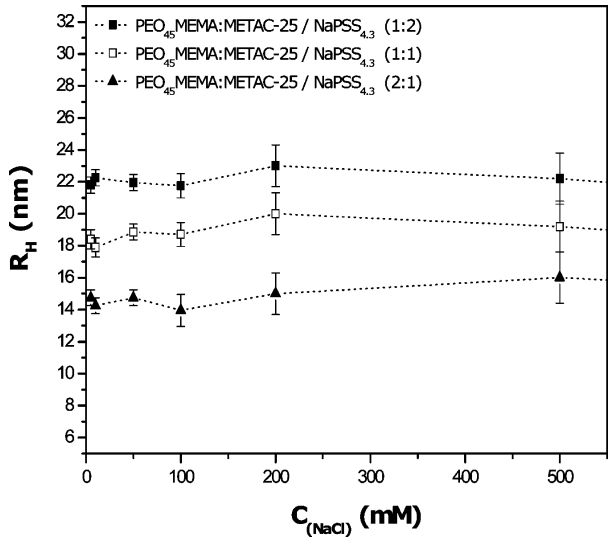

Figure 6. Hydrodynamic radius as a function of sodium chloride concentration for PECs of PEO_{45}MEMA:METAC-25/$PSS_{4.3}$.

where C is a constant (equal to 0.98 for linear (rather than parabolic) flow profile[60]), D_{app} the apparent diffusion coefficient, h, w, and l the height, width, and length of the flow channel, respectively, and F the volumetric flow rate. Due to the polydispersity of the bottle-brush polyelectrolyte, a direct comparison between experimental and theoretical values for k_m is difficult.[61] Thus, we instead take the approach to compare the variation in the measured value of k_m to the change in $D_{app}^{2/3}$ and plot the ratio $k_m/D_{app}^{2/3}$ in Figure 8. A constant value of this quantity means that the attachment probability is unaffected, whereas a decreased value demonstrates a decreased attachment probability.

The data in Figure 8 show that the value of $k_m/D_{app}^{2/3}$ decreases with PSS content in the PEC, and that this effect increases with increasing molecular weight of the PSS. This is not due to the increased size of the PEC, as this effect is taken into account in the factor $k_m/D_{app}^{2/3}$, but demonstrates that the adsorption probability of a PEC particle that collides with the surface decreases with PSS content and molecular weight.

The time evolution of the average layer thickness during the first 300 s of adsorption of the PEO_{45}MEMA:METAC-25/PSS_x and PEO_{45}MEMA:METAC-50/PSS_x complexes is shown in Figure 9.

Regardless of complex stoichiometry, the thickness of the layers formed by PEO_{45}MEMA:METAC-25 containing PECs is larger than that obtained for PECs containing PEO_{45}MEMA:-METAC-50. The layer thickness was found to decrease with PSS content and molecular weight. We note that the layer thickness reported by a DPI instrument is based on the assumption of a homogeneous layer. The accuracy of this assumption has been tested by adsorbing nanoparticles with known size, and it was found that the proper layer thickness was returned when the area coverage of the nanoparticles was larger than 17%.[62] Thus, the low thickness values obtained in the initial state of the adsorption should not be considered to reflect the height of the individual adsorbed molecules/PECs.

The adsorbed amount achieved from the different PEC containing solutions are plotted as a function of NaPSS molecular weight in Figure 10. The data illustrate that the adsorbed mass decreases when the NaPSS molecular weight is increased. This effect is pronounced independent of the PEC composition, and in terms of absolute values the decrease is most significant for positively charged complexes.

DISCUSSION

The Hydrodynamic Charge. The average number of charges carried by the polyelectrolytes used in this investigation is provided in Table 2. We note that the average bottle-brush polyelectrolyte contains a larger number of charges than NaPSS of low molecular weight (4.3 and 17 kDa), but less charges than the high molecular weight PSS (150 kDa). Thus, in the stoichiometric complexes, several low molecular weight PSS must be associated to each bottle-brush polymer, whereas several bottle-brush polyelectrolytes must be associated to each high molecular weight PSS. We note the polydispersity of the polymers, M_w/M_n is 1.1 for PSS and 2−3 for the bottle-brush polymers, which obviously is important for facilitating the formation of charge stoichiometric complexes at the 1:1 mixing ratio.

dx.doi.org/10.1021/la300365q | Langmuir 2012, 28, 6618−6631

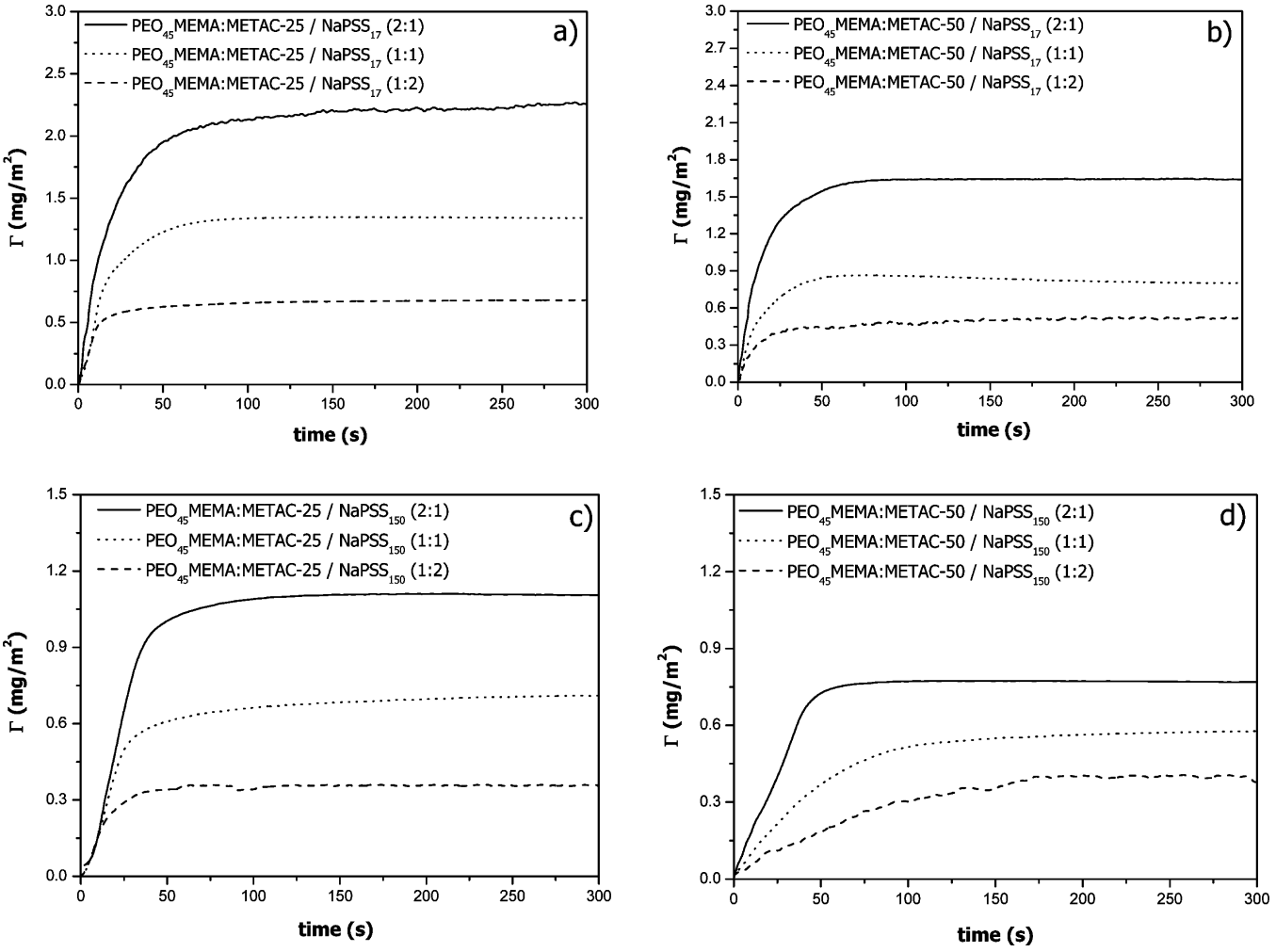

Figure 7. Adsorbed amount as a function of time for (a) $PEO_{45}MEMA:METAC\text{-}25/NaPSS_{17}$, (b) $PEO_{45}MEMA:METAC\text{-}50/NaPSS_{17}$, (c) $PEO_{45}MEMA:METAC\text{-}25/NaPSS_{150}$, and (d) $PEO_{45}MEMA:METAC\text{-}50/NaPSS_{150}$ complexes on silicon oxynitride. The aqueous solution contained 5 mM NaCl.

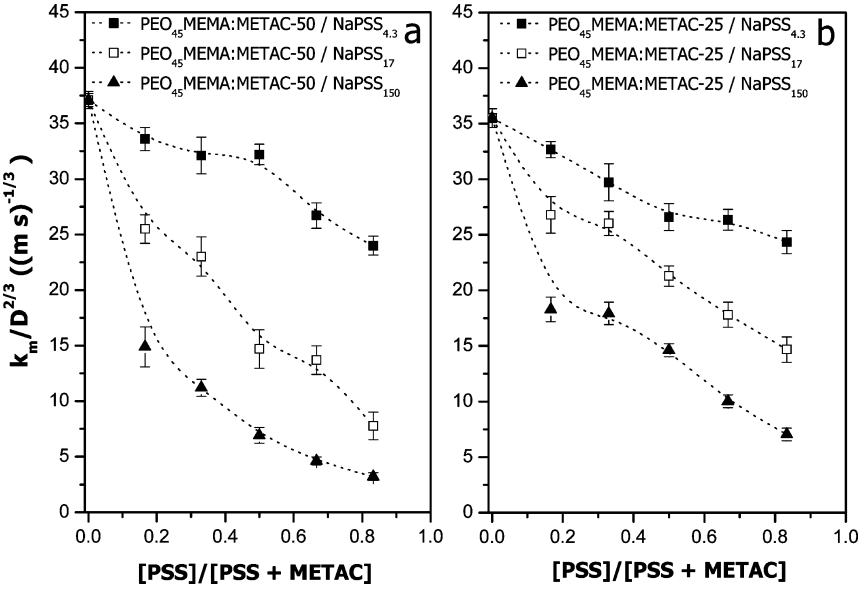

Figure 8. Quantity $k_m/D^{2/3}$, where k_m is the kinetic adsorption coefficient and D the diffusion coefficient, plotted as a function of PSS charge content for (a) $PEO_{45}MEMA:METAC\text{-}50/NaPSS_x$ and (b) $PEO_{45}MEMA:METAC\text{-}25/NaPSS_x$ complexes containing different molecular weight PSS.

dx.doi.org/10.1021/la300365q | *Langmuir* 2012, 28, 6618−6631

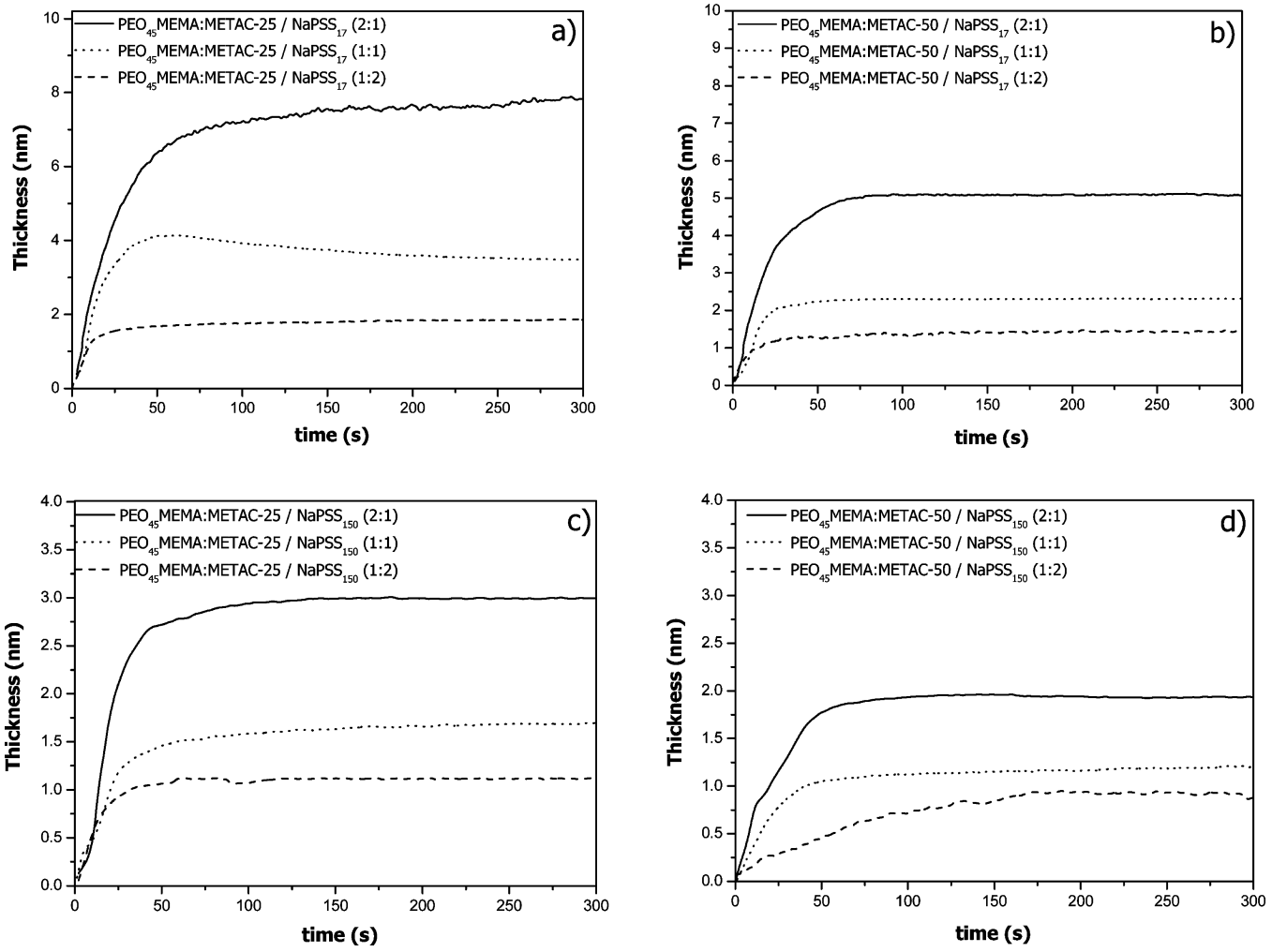

Figure 9. Layer thickness as a function of time for (a) $PEO_{45}MEMA:METAC\text{-}25/NaPSS_{17}$, (b) $PEO_{45}MEMA:METAC\text{-}50/NaPSS_{17}$, (c) $PEO_{45}MEMA:METAC\text{-}25/NaPSS_{150}$, and (d) $PEO_{45}MEMA:METAC\text{-}50/NaPSS_{150}$ complexes on silicon oxynitride. The aqueous solution contained 5 mM NaCl.

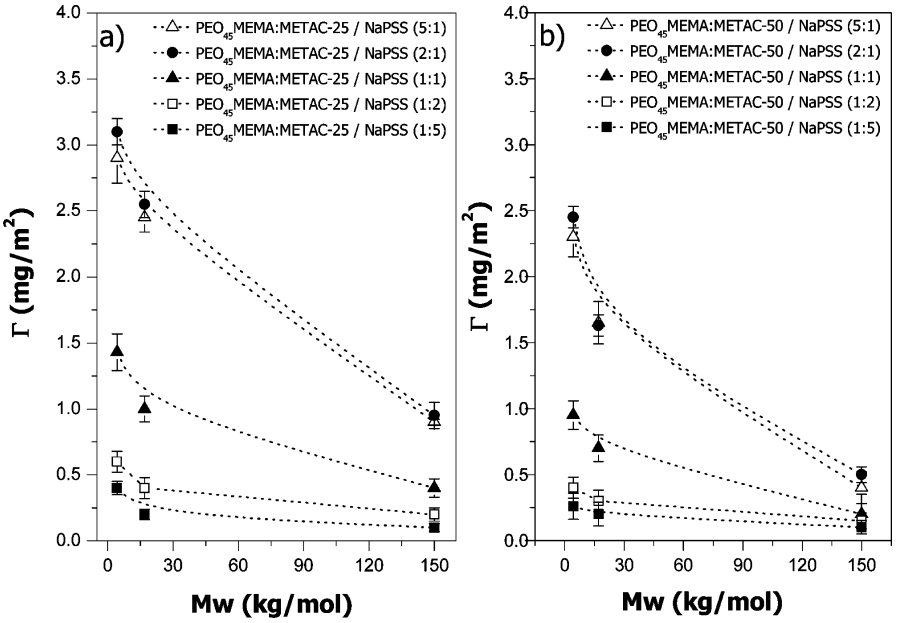

Figure 10. Adsorbed amount of complexes containing (a) $PEO_{45}MEMA:METAC\text{-}25$ and (b) $PEO_{45}MEMA:METAC\text{-}50$ as a function of PSS molecular weight. The solution contained 5 mM NaCl and 50 ppm of $PEO_{45}MEMA:METAC\text{-}25(50)$. The curved lines are plotted as guides for the eye.

dx.doi.org/10.1021/la300365q | *Langmuir* 2012, 28, 6618−6631

Table 2. Number of Charges Carried by the Average Polyelectrolyte

polyelectrolyte	no. of charges
PEO_{45}MEMA:METAC-25	102
PEO_{45}MEMA:METAC-50	298
$PSS_{4.3}$	21
PSS_{17}	82
PSS_{70}	338
PSS_{150}	725

The charge determined by an electrophoretic mobility measurement is equal to the charge located inside the volume defined by the liquid shear plane. Small ions are strongly accumulated close to highly charged polyelectrolytes,[63] and thus, the electrophoretic charge is expected to be significantly smaller than that of the polyion. This is also observed in our data where the hydrodynamic charge of PEO_{45}MEMA:-METAC-25 is about 60% of that of the polyion. The corresponding value for the more highly charged PEO_{45}MEMA:-METAC-50 is about 30%. The observation that a larger fraction of the counterions resides within the hydrodynamic volume for the more highly charged bottle-brush polyelectrolyte is consistent with theoretical predictions.[64] From Figure 2, we note that at the stoichiometric mixing ratio the mobility is zero, which suggests that the stoichiometry of the complex is the same as the stoichiometry of the mixture.

For the nonstoichiometric complexes, the measured magnitude of the charge of the PEC particles is always lower in magnitude than that calculated from eq 6 (Figure 11). For cationic complexes with low molecular weight PSS (4.3 and 17 kDa), the net charge contribution of the hydrodynamically coupled small ions decreases as charge neutrality is approached. Due to the strong electrostatic attraction between oppositely charged polyelectrolytes, it is plausible to suggest that also for the cationic PECs the complex stoichiometry is the same as in the mixture, as has been observed for linear polyelectrolytes using Monte Carlo simulations.[65] In excess of PSS, we observe the expected change of sign of the complex. However, the charge of the complex is much smaller than would be expected if all PSS was incorporated in the complex, and the charge difference between the 1:2 and 1:5 complexes is small. This suggests that all PSS are not incorporated in the complex but rather electrostatic repulsion between the negatively charged complex and the negative PSS puts a limit to the amount of anionic polyelectrolyte that can be incorporated. At this point, the hydrodynamic volume of the complex carries an excess of about 80 negative charges.

The nonstoichiometric complexes formed with high molecular weight PSS have significantly lower hydrodynamic charge than those formed by low molecular weight PSS (Figure 11). This is a consequence of their larger size (Figure 4) that results in a larger fraction of the counterions being included in the hydrodynamic volume of the complex.

Structure of PEC Particles. The bottle-brush polymers used in this investigation have been characterized by SAXS,[66] and similar bottle-brushes have also been investigated by SANS.[67] Their solution conformation can be described as being prolate with a short-axis, b, of about 4 nm, whereas the long-axis, a, is less well-defined due to the polydispersity of the polymer. The cross section radius of polylysine carrying side chains of PEO with molecular weight of 2 kDa was similarly found to be 4 nm by Feuz et al.[68]

The hydrodynamic radius of a prolate-shaped molecule is given by[69]

$$R_H = \frac{Q}{\ln\left(\frac{a+Q}{b}\right)} \tag{11}$$

where $Q = (a^2 - b^2)^{1/2}$.

By using 4 nm for the value of b and the measured R_H-values, the long-axis of the average bottle-brush polymer can be

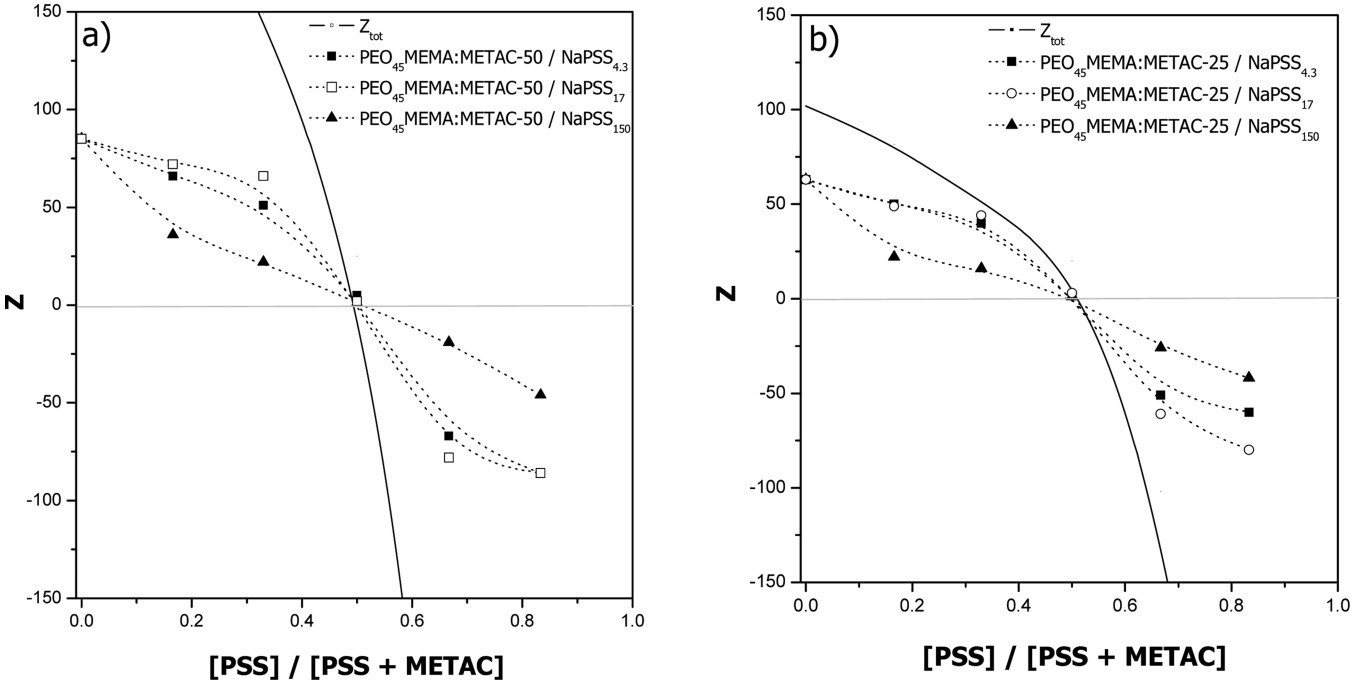

Figure 11. Number of charges (z) and total number of charges (z_{tot}) as a function of PSS content for (a) PEO_{45}MEMA:METAC-50/$NaPSS_x$ and (b) PEO_{45}MEMA:METAC-25/$NaPSS_x$ complexes. The concentration of the cationic polymer was fixed to 50 ppm.

dx.doi.org/10.1021/la300365q | Langmuir 2012, 28, 6618−6631

calculated to be about 13 nm for PEO_{45}MEMA:METAC-25 and 15 nm for PEO_{45}MEMA:METAC-50.

The cationic and stoichiometric complexes formed by PSS with molecular weight 4.3 kDa have only slightly larger hydrodynamic radius than the bottle-brush polymer alone (Figure 4), which suggests that the PSS is accommodated close to the backbone of the bottle-brush polymer. In contrast, the negatively charged complexes have higher R_H-values. For instance, for anionic PEO_{45}MEMA:METAC-50/$PSS_{4.3}$, the R_H-value is about 25 nm compared to 17 nm for the bottle-brush alone. This change corresponds to an increase in the long and short axis of the prolate by about 1.5 nm. This increase in dimension is suggested to be partly due to stretching of the PEO side chains due to the excluded volume repulsion exerted by the incorporated PSS, but also to the presence of some PSS molecules that extend from the bottle-brush backbone. Cationic PEO_{45}MEMA:METAC-50/PSS_{17} PECs have similar dimension as the anionic PEO_{45}MEMA:METAC-50/$PSS_{4.3}$ PECs. This demonstrates that even the first PSS_{17} molecules that are incorporated in the PECs partly extend from the backbone of the bottle-brush polyelectrolyte. The anionic PECs with PSS_{17} have a hydrodynamic radius of the order of 40 nm, which according to eq 9 means that the dimension of the prolate has increased by about 4 nm.

The total charge of PSS_{150} is larger than that of a typical bottle-brush polymer, and now we have the situation that several bottle-brush polymers are associated to one PSS molecule. Thus, we can no longer assume that the complex has a prolate shape. However, it is clear that the size of the complexes formed by PSS_{150} is larger than that for the PECs formed by the smaller PSS molecules (Figure 4), and the polydispersity of the PECs formed is also larger (Table 1). Just as for the complexes with low molecular weight PSS, the size of the anionic complexes is larger than that of the cationic ones.

We also note that the structural changes induced by addition of NaPSS to our bottle-brush polyelectrolytes, having a cationic backbone and uncharged side chains, appear to be less sophisticated compared to the case where the main chain is uncharged and the side chains charged. For the latter case, the work by Xu et al. on adsorbed PECs formed from bottle brushes with cationic side chains and NaPSS indicated transitions between wormlike, pearl-and-necklace, and globular fully collapsed PECs when low molecular weight NaPSS were used, and mainly the fully collapsed state was observed when large molecular weight NaPSS was added.[46]

Aggregation Behavior of PECs. It is well-known that PECs formed by linear polyelectrolytes aggregate when the electrostatic repulsion between the PECs is not sufficient to provide colloidal stability.[70] The PEO_{45} side chains in the cationic bottle-brush polyelectrolyte counteract this by providing steric stabilization. The side chain density of PEO_{45}MEMA:METAC-75 is lower than that for the other bottle-brush polymers, and thus, PEO_{45}MEMA:METAC-75/PSS PECs have limited stability (Figure 5). For PEO_{45}MEMA:METAC-75/$PSS_{4.3}$, colloidal stability is achieved for uncharged and cationic PECs but not for the anionic PECs. This is attributed to the presence of extended negatively charged PSS chains that facilitate bridging between different complexes, which is feasible considering that local positive patches are present also on net negatively charged complexes. Increasing the molecular weight of PSS leads to loss of the colloidal stability also for the uncharged and cationic PECs, since the probability of bridging increases with PSS molecular weight.

In contrast, the PEO_{45}MEMA:METAC-50/PSS and PEO_{45}MEMA:METAC-25/PSS PECs display excellent colloidal stability independent of the charge of the complex and on the molecular weight of PSS (up to 150 kDa). Thus, in these cases, the steric stabilization offered by the PEO_{45} side chains is sufficient, and the complexes remain stable in NaCl solutions up to a concentration of at least 0.5 M.

Driving Force for Adsorption. The cationic bottle-brush polymers used in this study adsorb to silica[71−73] and silicon oxynitride[61] due to electrostatic interactions between the backbone and the surface, as well as due to nonelectrostatic affinity between the PEO side chains and the substrate.[74,75] These polymers also adsorb to mica, but in this case adsorption is driven by only electrostatic forces.[51,74,75] Other studies, both theoretical and experimental, have demonstrated adsorption of structurally similar bottle-brush polymers to other oxide surfaces[76,77] and to nonpolar substrates.[78] The adsorption reported for the bottle-brush polymers in this work is consistent with previous results, where it has been shown that the backbone is not lying flat on the surface but more extended layers are formed.[61,71] In contrast, we found no detectable adsorption of PSS on silicon oxynitride.

The complexes formed can thus in principle adsorb through electrostatic interactions with the main chain and through the PEO_{45} side chains, whereas the PSS molecules within the complex are repelled from the surface. Thus, when a PEC collides with the surface, it can adsorb if the PEO_{45} side chains or the bottle-brush backbone encounter the surface, but not if the encounter occurs through the PSS chain. The likelihood of adsorption is thus expected to decrease with PSS content of the PEC and with increasing molecular weight of PSS, since these conditions favor extended PSS chains. The plots shown in Figure 8 show exactly these trends.

In our previous work, we showed by XPS that adsorbed layers formed by PEO_{45}MEMA:METAC-X/$PSS_{4.3}$ contain much less PSS than the complexes.[56] In fact, so little that hardly any PSS could be detected in the adsorbed layer. This finding demonstrates that the low molecular weight PSS desorbs from the complex during adsorption and that adsorption proceeds through a competitive process where negative surface sites compete with PSS for binding to the cationic sites on the bottle-brush polyelectrolyte. Provided the same mechanism prevails also for PECs formed using PSS with higher molecular weight, then one would expect the adsorbed layer to consist nearly exclusively of the bottle-brush polyelectrolyte and the layer thickness would then depend only on the adsorbed amount and not on from which PEC solution it was formed. This trend is indeed observed as illustrated in Figure 12, indicating that PSS desorbs from the complex during the PEC adsorption process.

The lower adsorbed amount obtained for higher PSS content in the PEC, and for higher molecular weight of PSS for a given PSS content, is then attributed primarily to a shift in the equilibrium between surface bound and complex bound bottle-brush polymers toward the complex bound state. This is consistent with the adsorption data shown in Figure 7, which demonstrate that a plateau value for the adsorption is reached for each PEC solution and thus the low adsorbed mass obtained for complexes with high PSS content is not due to slow adsorption kinetics.

Comparison with Other Studies. Our studies of PEC adsorption differ from those reported in other studies due to the presence of the PEO_{45} side chains that impose steric stabilization and strongly limit the size of the PECs formed.

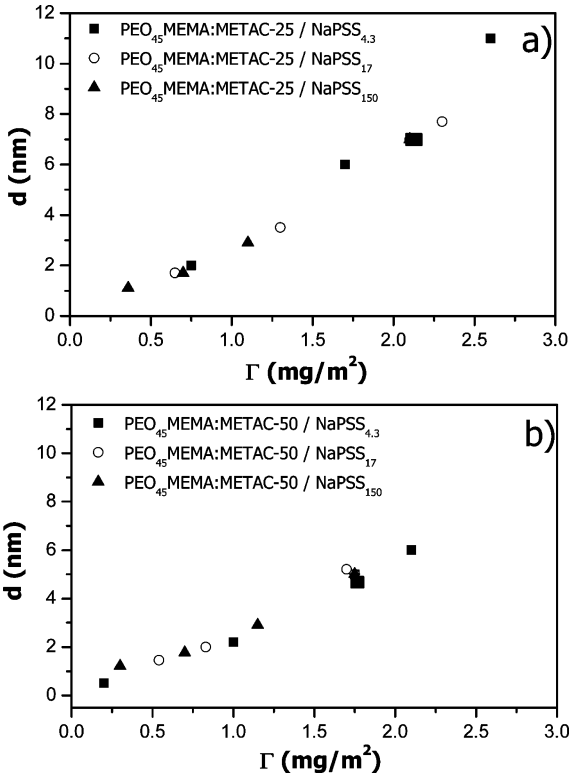

Figure 12. Thickness as a function of adsorbed amount for (a) $PEO_{45}MEMA:METAC-25/NaPSS_x$ and (b) $PEO_{45}MEMA:METAC-50/NaPSS_x$ complexes. The large square corresponds to data for the bottle-brush polymer alone.

The small size of our PECs facilitates removal of the anionic component upon adsorption, compared to the situation in large multichain PEC aggregates where disentanglement of one component has to be significantly slower. Considering this difference, it is not surprising that adsorption of large multichain aggregates follows a different route than that described in this report. For instance, Wågberg et al.[50] found the same dependence on the PEC stoichiometry, using poly(allyamine hydrochloride) and poly(acrylic acid), on the adsorption to negatively charged silica as reported by us in this Article. On the other hand, they found that the adsorbed mass increased with increasing molecular weight of the polyions incorporated in the PECs. This difference can be rationalized by loss of the anionic component during adsorption of our small PECs, but not (to the same extent) in the case of the large PECs employed by Wågberg et al.

CONCLUSIONS

Polyelectrolyte complexes were formed between a series of anionic linear and cationic bottle-brush polyelectrolytes. The effects of mixing ratio, concentration of the polyelectrolytes, charge density of the bottle-brush polyelectrolyte, and molecular weight of the anionic polyelectrolyte were explored.

Colloidally stable stoichiometric complexes could be formed when the PEO_{45} side chain density of the bottle-brush polyelectrolyte was sufficiently high. This was the case when equal or more than 50% of the main-chain segments carried a PEO_{45} side chain. The electrophoretic mobility data demonstrate that close to uncharged complexes are formed when equal amounts of charges from the PSS polyion and the bottle-brush polyion are added to the solution. The bottle-brush polymers adopt a prolate shape in solution, and the complexation of these bottle-brushes with $PSS_{4.3}$ and PSS_{17} leads to a moderate increase in the hydrodynamic size and no change in polydispersity, consistent with the picture that several small PSS molecules associate with the large bottle-brush. In contrast, when complexation occurs between PSS_{150} and the bottle-brush polymers, considerably larger PECs are formed and the polydispersity increases, consistent with several bottle-brush polymers associating with one high molecular weight PSS. In large excess of PSS, the combined data obtained from DLS and electrophoretic mobility measurements suggest that both negatively charged complexes and free PSS molecules exist in the solution.

Adsorption of stoichiometric and nonstoichiometric PECs on negatively charged silicon oxynitride was investigated by DPI. In general, the adsorbed amount decreases with increasing PSS content of the complex, and at a given PSS content with the molecular weight of the polyanion. Further, the thickness of the layer formed scales with the adsorbed amount, and the same master curve was observed independent of PSS molecular weight. This finding is rationalized by removal of a large fraction of the PSS from the complex during the adsorption process. The adsorbed mass achieved under a given condition is thus dictated by a competition between anionic surface sites and anionic sites on PSS for complexation with the cationic sites on the bottle-brush main chain. This equilibrium is shifted toward the complex side with increasing PSS content and increasing PSS molecular weight. The PSS content and molecular weight also influence the initial adsorption kinetics above that expected by the different sizes of the complexes. A higher PSS content and larger PSS molecular weight decrease the adsorption probability, which is due to the presence of extended PSS chains that counteract adsorption.

AUTHOR INFORMATION

Notes

The authors declare no competing financial interest.

ACKNOWLEDGMENTS

A.S. and P.M.C. acknowledge financial support from the Swedish Research Council. Dr. Ali Naderi is thanked for fruitful discussions and useful suggestions. This work was supported within the 7th European Community RTD Framework Program by the Marie Curie European Reintegration Grant, PE-NANOCOMPLEXES (PERG02-GA-2007-2249) and the Hungarian Scientific Research Fund OTKA H-07A 74230. I.V. is a Bolyai János fellow of the Hungarian Academy of Sciences that is gratefully acknowledged.

REFERENCES

(1) Michaels, A. S. Polyelectrolyte complexes. *Ind. Eng. Chem.* **1965**, *57*, 32−40.

(2) Philipp, B.; Dautzenberg, H.; Linow, K.-J.; Kötz, J.; Dawydoff, W. Polyelectrolyte-complexes - recent developments and open problems. *Prog. Polym. Sci.* **1989**, *14*, 91−172.

(3) Bucur, C. B.; Sui, Z.; Schlenoff, J. B. Ideal mixing in polyelectrolyte complexes and multilayers: Entropy driven assembly. *J. Am. Chem. Soc.* **2006**, *128*, 13690−13691.

(4) Ankerfors, C.; Ondaral, S.; Wågberg, L.; Ödberg, L. Using jet mixing to prepare polyelectrolyte complexes: Complex properties and their interaction with silicon oxide surfaces. *J. Colloid Interface Sci.* **2010**, *351*, 88−95.

(5) Eisenberg, H. Polyelectrolytes, 30 years later. *Biophys. Chem.* **1977**, *7*, 3−13.

(6) Schmitz, K. S. *Macro-ion charcaterization*; American Chemical Society: Washington, DC, 1993; Vol. *548*.
(7) Kötz, J.; Kosmella, S.; Beitz, T. Self-assembled polyelectrolyte systems. *Prog. Polym. Sci.* **2001**, *26*, 1199−1232.
(8) Thünemann, A. F.; Müller, M.; Dautzenberg, H.; Joanny, J.-F.; Löwen, H. Polyelectrolyte complexes. In *Polyelectrolytes with defined molecular architecture II*; Schmidt, M., Ed.; Springer-Verlag: Berlin, 2004; Vol. *166*, pp 113−171.
(9) Kabanov, V. A. Polyelectrolyte complexes in solution and in condensed phase. *Russ. Chem. Rev.* **2005**, *74*, 5−23.
(10) Mihai, M.; Dragan, E. S. Chitosan based nonstoichiometric polyelectrolyte complexes as specialized flocculants. *Colloids Surf., A* **2009**, *346*, 39−46.
(11) Petzold, G.; Mende, M.; Lunkwitz, K.; Schwarz, S.; Buchhammer, H.-M. Higher efficiency in the flocculation of clay suspensions by using combinations of oppositely charged polyelectrolytes. *Colloids Surf., A* **2003**, *218*, 47−57.
(12) Sukhishvili, S. A.; Kharlampieva, E.; Izumrudov, V. Weak polyelectrolyte multilayers and polyelectrolyte complexes meet. *Macromolecules* **2006**, *39*, 8873−8881.
(13) Bolto, B.; Gregory, J. Organic polyelectrolytes in water treatment. *Water Res.* **2007**, *41*, 2301−2324.
(14) Savage, N.; Diallo, M. S. Nanomaterials and water purification: Opportunities and challanges. *J. Nanoparticle Res.* **2005**, *7*, 331−342.
(15) Gärdlund, L.; Forsström, J.; Andreasson, B.; Wågberg, L. Influence of polyelectrolyte complexes on the strength properties of papers from unbleached kraft pulps with different yield. *Nord. Pulp Pap. Res. J.* **2005**, *20*, 36−42.
(16) Gärdlund, L.; Norgren, M.; Wågberg, L.; Marklund, A. The use of polyelectrolyte complexes (PEC) as strength additives for different pulps used for production of fine paper. *Nord. Pulp Pap. Res. J.* **2007**, *22*, 210−216.
(17) Moghimi, S. M.; Hunter, A. C.; Murray, J. C. Nanomedicine: current status and future prospects. *FASEB J.* **2005**, *19*, 311−330.
(18) Malmsten, M. Soft drug delivery systems. *Soft Matter* **2006**, *2*, 760−769.
(19) Izumrudov, V. A.; Galaev, I. Y.; Mattiasson, B. Polycomplexes - potential for bioseparation. *Bioseparation* **1998**, *7*, 207−220.
(20) Hartig, S. M.; Greene, R. R.; Dikov, M. M.; Prokop, A.; Davidson, J. M. Multifunctional nanoparticulate polyelectrolyte complexes. *Pharm. Res.* **2007**, *24*, 2353−2369.
(21) Tsuchida, E.; Osada, Y.; Sanada, K. Interactions of poly(styrene sulfonate) with polycations carrying charges in the backbone. *J. Polym. Sci., Part A* **1972**, *10*, 3397−3404.
(22) Kramer, G.; Buchhammer, H.-M.; Lunkwitz, K. Surface modification by polyelectrolyte complexes: Influence of different components and substrates. *Colloids Surf., A* **1997**, *122*, 1−12.
(23) Dautzenberg, H.; Gao, Y.; Hahn, M. Formation, structure, and temperature behavior of polyelectrolyte complexes between ionically modified thermosensitive polymers. *Langmuir* **2000**, *16*, 9070−9081.
(24) Zintchenko, A.; Rother, G.; Dautzenberg, H. Transition highly aggregated complexes - soluble complexes via polyelectrolyte exchange reactions: Kinetics, structural changes, and mechanism. *Langmuir* **2003**, *19*, 2507−2513.
(25) Bakeev, K. N.; Izumrudov, V. A.; Kuchanov, S. I.; Zezin, A. B.; Kabanov, V. A. Kinetics and mechanism of interpolyelectrolyte exchange and addition reactions. *Macromolecules* **1992**, *25*, 4249−4254.
(26) Hayashi, Y.; Ullner, M.; Linse, P. Complex formation in solutions of oppositely charged polyelectrolytes at different compositions and salt content. *J. Phys. Chem. B* **2003**, *107*, 8198−8207.
(27) Hayashi, Y.; Ullner, M.; Linse, P. Oppositely charged polyelectrolytes. Complex formation and effects of chain asymmetry. *J. Phys. Chem. B* **2004**, *108*, 15266−15277.
(28) Rydén, J.; Ullner, M.; Linse, P. Monte Carlo simulations of oppositely charged macroions in solution. *J. Chem. Phys.* **2005**, *123*, 034909.
(29) Kramarenko, E. Y.; Khokhlov, A. R.; Reineker, P. Micelle formation in a dilute solution of block copolymers with polyelectrolyte block complexed with oppositely charged linear chain. *J. Chem. Phys.* **2003**, *119*, 4945−4953.
(30) Kramarenko, E. Y.; Pevnaya, O. S.; Khokhlov, A. R. Stoichiometric polyelectrolyte complexes as comb copolymers. *J. Chem. Phys.* **2005**, *122*, 084902.
(31) Cohen Stuart, M. A.; Hofs, B.; Voets, I. K.; de Kaizer, A. Assembly of polyelectrolyte-containing block copolymers in aqueous media. *Curr. Opin. Colloid Interface Sci.* **2005**, *10*, 30−36.
(32) Sotiropoulou, M.; Bokias, G.; Staikos, G. Water-soluble complexes through Coulombic interactions between bovine serum albumin and anionic polyelectrolytes grafted with hydrophilic nonionic side chains. *Biomacromolecules* **2005**, *6*, 1835−1838.
(33) Kabanov, A. V.; Bronich, T. K.; Kabanov, V. A.; Yu, K.; Eisenberg, A. Soluble Stoichiometric complexes from poly(N-ethyl-4-vinylpyridinium) cations and poly(ethylene oxide)-block-polymethacrylate anions. *Macromolecules* **1996**, *29*, 6797−6802.
(34) Mori, H.; Müller, A. H. E. New polymeric architectures with (meth)acrylic acid segments. *Prog. Polym. Sci.* **2003**, *28*, 1403−1439.
(35) Matralis, A.; Sotiropoulou, M.; Bokias, G.; Staikos, G. Water-soluble stoichiometric polyelectrolyte complexes based on cationic comb-type copolymers. *Macromol. Chem. Phys.* **2006**, *207*, 1018−1025.
(36) Larin, S. V.; Pergushov, D. V.; Xu, Y.; Darinskii, A. A.; Zezin, A. B.; Müller, A. H. E.; Borisov, O. V. Nano-patterned structures in cylindrical polyelectrolyte brushes assembled with oppositely charged polyions. *Soft Matter* **2009**, *5*, 4938−4943.
(37) Shovsky, A.; Varga, I.; Makuska, R.; Claesson, P. M. Formation and stability of water-soluble molecular polyelectrolyte complexes: Effects of charge density, mixing ratio, and polyelectrolyte concentration. *Langmuir* **2009**, *25*, 6113−6121.
(38) Shovsky, A.; Varga, I.; Makuska, R.; Claesson, P. M. Formation and stability of soluble stoichiometric polyelectrolyte complexes: Effects of charge density and polyelectrolyte concentration. *J. Dispersion Sci. Technol.* **2009**, *30*, 980−988.
(39) Dedinaite, A. Biomimetic lubrication. *Soft Matter* **2012**, *8*, 273−284.
(40) Dedinaite, A. Interfacial properties of mucins. In *Encyclopedia of Surface and Colloid Science*, 2nd ed.; Taylor and Francis: London, 2010; pp 1−17.
(41) Lee, H.; Pietrasik, J.; Sheiko, S. S.; Matyjaszewski, K. Stimuli-responsive molecular brushes. *Prog. Polym. Sci.* **2010**, *35*, 24−44.
(42) Ruthard, C.; Maskos, M.; Kolb, U.; Gröhn, F. Finite-size networks from cylindrical polyelectrolyte brushes and porphyrins. *Macromolecules* **2009**, *42*, 830−840.
(43) Xu, Y.; Bolisetty, S.; Ballauff, M.; Müller, A. H. E. Switching the morphology of cylindrical brushes by ionic supramolecular inclusion complexes. *J. Am. Chem. Soc.* **2009**, *131*, 1640−1641.
(44) Lienkamp, K.; Noé, L.; Breniaux, M.-H.; Lieberwirth, I.; Groehn, F.; Wegner, G. Synthesis and characterization of end-functionalized cylindrical polyelectrolyte brushes from poly(styrene sulfonate). *Macromolecules* **2007**, *40*, 2486−2502.
(45) Störkle, D.; Duschner, S.; Heimann, N.; Maskos, M.; Schmidt, M. Complex formation of DNA with oppositely charged polyelectrolytes of different chain topology: Cylindrical brushes and dendrimers. *Macromolecules* **2007**, *40*, 7998−8006.
(46) Xu, Y.; Borisov, O. V.; Ballauff, M.; Müller, A. H. E. Manipulating the morphologies of cylindrical polyelectrolyte brushes by forming interpolyelectrolyte complexes with oppositely charged linear polyelectrolytes: An AFM study. *Langmuir* **2010**, *26*, 6919−6926.
(47) Blockhus, A. M.; Djurhuus, K. Adsorption of poly(styrene sulfonate) of different molecular weight on a-alumina: Effect of added sodium dodecyl sulfate. *J. Colloid Interface Sci.* **2006**, *296*, 64−70.
(48) Saarinen, T.; Österberg, M.; Laine, J. Properties of cationic polyelectrolyte layers adsorbed on silica and cellulose surfaces studied by QCM-D - effect of polyelectrolyte charge density and molecular weight. *J. Dispersion Sci. Technol.* **2009**, *30*, 969−979.
(49) Gärdlund, L.; Wågberg, L.; Gernandt, R. Polyelectrolyte complexes for surface modification of wood fibres II. Influence of

complexes on wet and dry strength of paper. *Colloids Surf., A* **2003**, *218*, 137−149.
(50) Ondaral, S.; Ankerfors, C.; Ödberg, L.; Wågberg, L. Surface-induced rearrangements of polyelectrolyte complexes: Influence of complex composition on adsorbed layer properties. *Langmuir* **2010**, *26*, 14606−14614.
(51) Naderi, A.; Iruthayaraj, J.; Vareikis, A.; Makuska, R.; Claesson, P. M. Surface properties of bottle-brush polyelectrolytes on mica: Effect of side chain- and charge density. *Langmuir* **2007**, *23*, 12222−12232.
(52) Schmitz, K. S. *An introduction to dynamic light scattering by macromolecules*; Academic Press: London, 1990.
(53) Brown, J. C.; Pusey, P. N. Measurement of diffusion coefficients of polydisperse solutes by photon correlation spectroscopy. *J. Phys. D* **1974**, *7*, L31−L35.
(54) Swann, M. J.; Peel, L. L.; Carrington, S.; Freeman, N. J. Dual-polarization interferometry: an analytical technique to measure changes in protein structure in real time, to determine the stoichiometry of binding events, and to differentiate between specific and nonspecific interactions. *Anal. Biochem.* **2004**, *329*, 190−198.
(55) Cross, G. H.; Reeves, A.; Brand, S.; Popplewell, J. F.; Peel, L. L.; Swann, M. J.; Freeman, N. J. A new quantitative optical biosensor for protein characterisation. *Biosens. Bioelectron.* **2003**, *19*, 383−390.
(56) Shovsky, A.; Bijelic, G.; Varga, I.; Makuska, R.; Claesson, P. M. Adsorption characteristics of stoichiometric and non-stoichiometric polyelectrolyte complexes on silicon oxynitride surfaces. *Langmuir* **2011**, *27*, 1044−1050.
(57) Naderi, A.; Claesson, P. M. Association between poly(vinylamine) and sodium dodecyl sulfate: Effects of mixing protocol, blending procedure and salt concentration. *J. Dispersion Sci. Technol.* **2005**, *26*, 329−340.
(58) Naderi, A.; Claesson, P. M.; Bergström, M.; Dedinaite, A. Trapped non-equilibrium states in aqueous solutions of oppositely charged polyelectrolytes and surfactants: effects of mixing protocol and salt concentration. *Colloids Surf., A* **2005**, *253*, 83−93.
(59) Glaser, R. W. Antigen-antibody binding and mass transport by convection and diffusion to a surface: A two-dimensional computer model of binding and dissociation kinetics. *Anal. Biochem.* **1993**, *213*, 152−161.
(60) Sjölander, S.; Urbaniczky, C. Integrated fluid handling system for biomolecular interaction analysis. *Anal. Chem.* **1991**, *63*, 2338−2345.
(61) Bijelic, G.; Shovsky, A.; Varga, I.; Makuska, R.; Claesson, P. M. Adsorption characteristics of brush polyelectrolytes on silicon oxynitride revealed by dual polarization interferometry. *J. Colloid Interface Sci.* **2010**, *348*, 189−197.
(62) Cross, G. H.; Reeves, A.; Brand, S.; Swann, M. J.; Peel, L. L.; Freeman, N. J.; Lu, J. R. The metrics of surface adsorbed small molecules on the Young's fringe dual-slab waveguide interferometer. *J. Phys D* **2004**, *37*, 74−80.
(63) Manning, G. S. Limiting laws and counterion condensation in polyelectrolyte solutions I. Colligative properties. *J. Chem. Phys.* **1969**, *51*, 924−933.
(64) Dobrynin, A. V.; Rubinstein, M. Theory of polyelectrolytes in solutions and at surfaces. *Prog. Polym. Sci.* **2005**, *30*, 1049−1118.
(65) Hayashi, Y.; Ullner, M.; Linse, P. A Monte Carlo study of solutions of oppositely charged polyelectrolytes. *J. Chem. Phys.* **2002**, *116*, 6836−6845.
(66) Dedinaite, A.; Bastardo, L.; Oliveira, C. P.; Pedersen, J. S.; Claesson, P. M.; Vareikis, A.; Makuska, R. *Solution properties of bottle-brush polyelectrolytes*, Proceed. Baltic Polymer Symp., Druskininkai, Lithuania; Makuska, R., Romaskevic, T., Eds.; Vinius University: Druskininkai, Lithuania, 2007; pp 112−116.
(67) Bastardo, L.; Iruthayaraj, J.; Lundin, M.; Dedinaite, A.; Vareikis, A.; Makuska, R.; van der Wal, A.; Furó, I.; Garamus, V. M.; Claesson, P. M. Soluble complexes in aqueous mixtures of low charge density comb polyelectrolytes and oppositely charged surfactants probed by scattering and NMR. *J. Colloid Interface Sci.* **2007**, *312*, 21−33.
(68) Feuz, L.; Strunz, P.; Geue, T.; Textor, M.; Borisov, O. V. Conformation of poly(L-lysine)-*graft*-poly(ethylene glycol) molecular brushes in aqueous solution studied by small-angle neutron scattering. *Eur. Phys. J.* **2007**, *E23*, 237−245.
(69) van de Sande, W.; Persoons, A. The size and shape of macromolecular structures: determination of the radius, the length and the persistance length of rod-like micelles of dodecyldimethylammonium chloride and bromide. *J. Phys. Chem.* **1985**, *89*, 404−406.
(70) Mihai, M.; Dragan, E. S.; Schwarz, S.; Janke, A. Dependency of particle sizes and colloidal stability of polyelectrolyte complex dispersions on polyanion structure and preparation mode investigated by dynamic light scattering and atomic force microscopy. *J. Phys. Chem. B* **2007**, *111*, 8668−8675.
(71) Iruthayaraj, J.; Olanya, G.; Claesson, P. M. Viscoelastic properties of adsorbed bottle-brush polymer layers studied by quartz crystal microbalance-dissipation measurements. *J. Phys. Chem. C* **2008**, *112*, 15028−15036.
(72) Iruthayaraj, J.; Poptoshev, E.; Vareikis, A.; Makuska, R.; van der Wal, A.; Claesson, P. M. Adsorption of low charge density polyelectrolyte containing poly(ethylene oxide) side chains on silica: Effects of ionic strength and pH. *Macromolecules* **2005**, *38*, 6152−6160.
(73) Olanya, G.; Iruthayaraj, J.; Poptoshev, E.; Makuska, R.; Vareikis, A.; Claesson, P. M. Adsorption characteristics of bottle-brush polymers on silica: Effect of side chain and charge density. *Langmuir* **2008**, *24*, 5341−5349.
(74) Linse, P.; Claesson, P. M. Modeling of bottle-brush polymer adsorption onto mica and silica surfaces. *Macromolecules* **2009**, *42*, 6310−6318.
(75) Linse, P.; Claesson, P. M. Modeling of bottle-brush polymer adsorption onto mica and silica surfaces: Effect of side-chain length. *Macromolecules* **2010**, *43*, 2076−2083.
(76) Pasche, S.; De Paul, S. M.; Vörös, J.; Spence, N. D.; Textor, M. Poly(L-lysine)-*graft*-poly(ethylene glycol) assembled monolayers on niobium oxide surfaces: A quantitative study on the influence of polymer interfacial architecture on resistance to protein adsorption by ToF-SIMS and in situ OWLS. *Langmuir* **2003**, *19*, 9216−9225.
(77) Feuz, L.; Leermakers, F. A. M.; Textor, M.; Borisov, O. V. Adsorption of molecular brushes with polyelectrolyte backbones onto oppositely charged surfaces: A self-consistent field theory. *Langmuir* **2008**, *24*, 7232−7244.
(78) Lee, S.; Spence, N. D. Adsorption properties of poly(L-lysine)-*graft*-poly(ethylene glycol) (PLL-*g*-PEG) at a hydrophobic interface: Influence of tribological stress, pH, salt concentration and polymer molecular weight. *Langmuir* **2008**, *24*, 9479−9488.